Confirm co-authorship of submission to Kuwait Journal of Science

Eksternal

Kotak Masuk

nal@editorialmanager.com>

Sen, 30 Okt 2023, 07.24

This is an automated message

Journal: Kuwait Journal of Science
Title: Organobentonite Fabrication by Octadecylamine Intercalation in Hydrothermal as Direct Dye Wastewater Adsorbent
Corresponding Author: Prof. Dr.rer.nat. Risfidian Mohadi
Co-Authors: Yusuf Mathiinul Hakim; Mardiyanto Mardiyanto, Dr.rer.nat.; Idha Royani, Dr.
Manuscript Number: KJS-D-23-02294

Dear Mardiyanto Mardiyanto,

Prof. Dr.rer.nat. Risfidian Mohadi submitted this manuscript via Elsevier's online submission system, Editorial Manager, and you have been listed as a Co-Author of this submission.

Elsevier asks Co-Authors to confirm their consent to be listed as Co-Author and track the papers status. In order to confirm your connection to this submission, please click here to confirm your co-authorship:

Yes, I am affiliated.

If you have not yet registered for the journal on Editorial Manager, you will need to create an account to complete this confirmation. Once your account is set up and you have confirmed your status as Co-Author of the submission, you will be able to view and track the status of the submission as it goes through the editorial process by logging in at https://www.editorialmanager.com/kjs/

If you did not co-author this submission, please contact the Corresponding Author directly at risfidian.mohadi@unsri.ac.id

Thank you,

Kuwait Journal of Science

More information and support

FAQ: What is Editorial Manager Co-Author registration?
https://service.elsevier.com/app/answers/detail/a_id/28460/supporthub/publishing/kw/co-author+editorial+manager/

You will find information relevant for you as an author on Elsevier’s Author Hub: https://www.elsevier.com/authors
FAQ: How can I reset a forgotten password?

https://service.elsevier.com/app/answers/detail/a_id/28452/supporthub/publishing/
For further assistance, please visit our customer service
site: https://service.elsevier.com/app/home/supporthub/publishing/
Here you can search for solutions on a range of topics, find answers to frequently asked questions, and learn more about Editorial Manager via interactive tutorials. You can also talk 24/7 to our customer support team by phone and 24/7 by live chat and email

#AU_KJS#

To ensure this email reaches the intended recipient, please do not delete the above code

---

Manuscript pada halaman di bawah ini

Organobentonite fabrication assisted by surfactant octadecylamine intercalation under hydrothermal/solvothermal condition for effective direct yellow dye removal

Yusuf Mathiinul Hakim [a], Mardiyanto [b], Idha Royani [c,d], Risfidian Mohadi [a,d,*]

[a] *Doctoral Program of Natural Science, Graduate School of Mathematics and Natural Sciences, Faculty of Mathematics and Natural Sciences, Sriwijaya University, Palembang, 30139, South Sumatera, Indonesia*

[b] *Pharmaceutical Department, Faculty of Mathematics and Natural Sciences, Sriwijaya University, Palembang, 30139, South Sumatera, Indonesia*

[c] *Department of Physics, Faculty of Mathematics and Natural Sciences, Sriwijaya University, Palembang, 30139, South Sumatera, Indonesia*

[d] *Magister Program of Materials Science, Graduate School of Sriwijaya University, Palembang, 30139, South Sumatera, Indonesia*

E-mail addresses: yusufmathiinul191@gmail.com (Y.M. Hakim), mardiyanto@mipa.unsri.ac.id (Mardiyanto), idharoyani@unsri.ac.id (I. Royani), risfidianmohadi@unsri.ac.id .

ABSTRACT

This study utilizes a hydrothermal-solvothermal method to facilitate the fabrication of organobentonite (OB) by intercalating the surfactant octadecylamine (ODA) using several solvents (water (OB-Aq), ethanol (OB–Et), and mix 50% water/ethanol (OB-Aq/Et)). The physicochemical features of the materials were investigated using X-ray diffraction, Fourier transform infrared, scanning electron microscopy, Brunauer-Emmett-Teller surface analyzer, and thermogravimetry differential thermal analysis characterization. The study of structural properties found that surfactant intercalation transformed the basal spacing. This was shown by a lower x-ray diffraction value of 2θ at <6° and the presence of peeled-off layers in the scanning electron microscope image. The thermogravimetry analysis and regeneration adsorption evaluated the structural stability of OB, demonstrating its capacity to withstand temperatures up to 300 °C and undergo three cycles of adsorption. In addition, the adsorption processes on direct yellow are mainly characterized by the pseudo-first-order kinetic and Langmuir isotherm models. The interaction between alumina-silica bentonite and ODA chains in this investigation influenced the adsorption mechanism. The adsorption system is influenced by pH, temperature, and ion competition, which can induce the disintegration of the direct yellow structure from the surfaces of the adsorbent. The mesoporous structures obtained have the highest Langmuir chemisorption capacities for OB-Aq, OB-Et, and OB-Aq/Et, with values of 270.27 mg/g, 108.696 mg/g, and 2000 mg/g, respectively. This work suggests using an efficient method to fabricate OB for anionic dyes removal, specifically direct yellow.

1. Introduction

Clean water access has gained global attention due to quality and quantity issues (UNESCO World Water Assessment Programme et al., 2023). A number of factors contribute to this issue, such as water access blockages caused by human conflict and water pollution from improper wastewater treatment in the textile, pharmacy, and agriculture industries. For instance, the human conflict in Palestine has caused per capita access to clean water to be estimated at only 56 L per day (or even less) due to leaks in water networks and restrictions on water access in the region (Yaqoub, 2023). In another case of water pollution, a modeling study explains that the pollution will expose more than 5.5 billion people in the world to polluted water by 2100 (Tozer, 2023). The post-accumulation of hazardous and undegradable pollutants, such as medical reactive compounds, pesticides, heavy metals, and synthetic dyes, can trigger mutagenic and carcinogenic phenomena (Vats et al., 2022), (Garg and Chopra, 2022), (Hemashenpagam and Selvajeyanthi, 2023). Furthermore, direct yellow (DY), a common anionic synthetic dye in the textile industry, contains an aromatic amine group (azo structure) as a waste by-product, which poses a carcinogenic threat (Alzain et al., 2023), (Khezrianjoo, 2019).

Treatment of dye wastewater pollutants is demanding depending on the methods and materials. Economical, high-capacity, and stable materials are unique features for nominating the fittest method. The generally known methods are adsorption, catalytic degradation, bio- removal, chemical precipitation, and others (Hakim et al., 2023a). Adsorption has emerged as a dependable and efficient approach for treating large quantities of wastewater. Unfortunately, adsorption has drawbacks such as instability, low capacity, and reusability for several adsorbents (Rashid et al., 2021). The appeal of nature-based adsorbents stems from their ability to overcome the limitations of conventional adsorbents through a variety of modification options. Clay minerals, as a nature-based material, are widely known for the adsorption features of swelling and reactive-layered surfaces. Furthermore, clay is an abundant mineral in the environment; thus, it has a low hazardous impact and risk of use (Barakan and Aghazadeh, 2021).

Bentonite is a type of clay mineral that is composed of negatively charged tetrahedra-silica layers that surround an octahedra-alumina layer. The basal spacing is characterized by the presence of exchangeable inorganic cations, which contribute to the material's ability to expand and adsorb substances (Hakim et al., 2023b). There are various ways to improve this material's properties, such as acid and thermal activation, intercalation, polymerization, and compositing schemes (Priatna et al., 2023).

Intercalation becomes the finest method for refining bentonite structures since it triggers wide-range basal spacing lifting. Nevertheless, bentonite possesses inherent hydrophilic properties and must undergo modification in order to become hydrophobic for effective utilization in the elimination of organic wastes (Qi et al., 2023). Salihi et al. (Çalıs¸kan Salihi et al., 2023) discovered that the intercala- tion of dodecyl-trimethylammonium bromide (DTAB) with bentonite enhanced paracetamol's adsorptive capacity, resulting in a Q_{max} value of 32.4 mg/g. According to De Morais Pinos et al. (de Morais Pinos et al., 2022), cetyltrimethylammonium bromide (CTAB) intercalation at bentonite only provides the Q_{max} for rhodamine B at 0.98 mg/g. Ac- cording to Taibi et al. (2023), the bentonite's Q_{max} was 31.49 mg/g after intercalating with cetyltrimethylammonium bromide (CTAB) as an orange G dye adsorbent.

As previous research has shown that the natural bentonite Q_{max} is limited, we now present a method to fabricate an organobentonite (OB) adsorbent using octadecylamine (ODA) surfactant as a high-density intercalant and analyze how the Q_{max} improves the adsorption of an anionic dye. In this study, we introduce the hydrothermal/solvothermal (HT/ST) method as a work method on the intercalation of surfactant ODA in different solvents including water, ethanol, and a 50% water/ ethanol mixture to improve the OB properties such as adsorption ca- pacity and stability. The HT/ST process is widely recognized as a gentle chemical method that ensures the resulting product has a high level of crystallinity and purity (Feng and Li, 2017).

The authors' review of the literature reveals a dearth of reports on the impact of HT/ST intercala- tion in preparing suitable bentonite-based adsorbents for dye waste- water. X-ray diffraction (XRD), Fourier transform infrared (FTIR), scanning electron microscopy (SEM), Brunauer-Emmett-Teller (BET) surface analyzer, and thermogravimetry differential thermal analysis (TG-DTA) are used to investigate the physicochemical properties. The work evaluates the adsorption of direct yellow dye using kinetic, isotherm, and thermodynamic parameters. This work also proposes the adsorption mechanism for OB.

2. Materials and methods

2.1. Chemicals

All chemicals are in pure grade and directly used, including sodium chloride (NaCl, 58.44 g/mol), ammonium chloride (NH_4Cl, 53.49 g/ mol), octadecylamine (ODA, $C_{18}H_{39}N$, 269.51 g/mol), sodium hydrox- ide (NaOH, 40 g/mol), and ethanol 97% (Et, C_2H_5OH, 46.07 g/mol), which were purchased from Sigma Aldrich. The 37% chloride acid (HCl, 36.46 g/mol) was purchased from Mallinckrodt AR. The distilled water (Aq) was purchased from Bratachem Corp. The direct yellow (DY, $C_{26}H_{18}N_4Na_2O_8S_2$) was imported from the local textile business in Palembang, Indonesia.

The primary material, clay bentonite (CB, imported from Pacitan, Indonesia), was previously activated by preparing CB (100 g) dispersion in a saturated NaCl solution (333 mL) at 600 rpm for 120 min, then filtered and re-dispersed in a similar condition. Finally, the secondary dispersion was HT at 105 °C for 12 h and washed with boiled Aq. The final residue was oven-dried at 105 °C for 12 h, grounded to 200 mesh, and denoted as Na–B.

2.2. *Organobentonite fabrication and characterization*

Organobentonite fabrication was prepared by dispersing Na–B (100 g) in a saturated NH_4Cl solution (333 mL) at 600 rpm for 120 min, then filtering it to be re-dispersed in the same condition. The secondary dispersion was HT at 105 °C for 12 h and washed with boiled Aq. The final residue was oven-dried at 105 °C for 12 h, grounded to 200 mesh, and denoted as NH–B.

The surfactant intercalation was carried out by preparing Na–B (1 g) dispersion in ODA solution (solution composition is 1:1 w/w% of ODA to Na–B in 200 mL solvents (solvent: Aq, Et, and Aq/Et 50%)) for 10 min at 300 rpm stirred and sonicated, followed by rapid stirring at 600 rpm for 30 min. The dispersion was HT/ST at 105 °C for 12 h, washed using Et and Aq, and then oven-dried at 80 °C for 12 h. The material was grounded to 200 mesh and named according to the solvents: OB-Aq, OB-Et, and OB-Aq/Et. Fabricated materials were characterized using XRD Rigaku Mini-flex 600 in 2θ range 5–80°, FTIR Shimadzu Prestige-21 in scan range 400–4000 cm^{-1}, surface analyzer Quantachrome TouchWin v1.22 at 77.35K by BET model, SEM JSM-7800F JEOL at 5 kV under 8000 magnification, and TG-DTA Rigaku

Thermo Plus EVO2 8122 under air condition between 25 and 500 °C for 10–15 mg samples. The filtrate (DY solution) concentration was analyzed with $\lambda = 400.2$ nm using the Spectrophotometer BK-UV 1800-PC.

2.3. Adsorption works

We initiated the point zero charge (pH_{pzc}) analysis and conducted the adsorption process on series works in the following steps: NaCl 0.1 M (20 mL) series were prepared in a pH range of 2–11 (pH adjusted by HCl and NaOH 0.1 M) and used in 12 h of adsorption by 20 mg of fabricated adsorbents. The initial and final pHs were measured. The DY adsorption in an aqueous solution was conducted using parameters of pH optimum, kinetics, isotherm, and thermodynamics. The adsorption step was car- ried out in a system of 20 mg adsorbent in 50 mg/L of DY solution (20 mL) under variables of pH-adjusted (2–11), contact time (10–180 min) temperature (30–70 °C), and initial concentration (100–200 mg/L). The regeneration process was carried out in the presence of 50 mg/L of DY solution for 120 min of adsorption, then desorbed by ultrasonication treatment for 15 min. The adsorption capacity (Q_t, mg/g) was calculated by the equation:

$$Q = \frac{(C_0 - C_t)}{W} V$$

Where C_0 and C_t are DY's concentration at initial and specific time (t), respectively (mg/L), then V and W are adsorbate volume (L) and adsorbent dose (g).

3. Results and discussion

3.1. Characterization

X-Ray diffraction (XRD) is a common tool in mineral characteriza- tion because it specifies material crystallinity (Cuevas et al., 2022). XRD patterns for OB show a clear transformation after HT/ST treatment of the surfactant ODA intercalation. The basal spacing lifting induced a structural rearrangement, leading to a decrease in the 2θ value from 5.54° (CB) to 5.24° (OB-Aq), 5.8° (OB–Et), and 4.88° (OB-Aq/Et) (see Fig. 1b) (Iwasaki, 2020). The values of 6°, 20°, and 36° at 2θ are attributed to the (002) and (110) phases of montmorillonite crystal (JCPDS file no. 79–1910). The basal spacing on clay minerals is generally identified from 2θ of XRD at 5–15° (Segad et al., 2010). During the process of intercalation, the contact between the montmorillonite mineral structure and ODA chains is maintained by HT/ST processes. This interaction affects the structure of the bentonite layers, causing them to peel, and ultimately leads to a higher peak in montmorillonite crystallinity (Zhong et al., 2022).

In this case, the direction of the intercalant arrangement depends on the surfactant solubility in a solvent (Laipan et al., 2020). Water-based solvents render the surfactant ODA insoluble, thereby creating a well-ordered or symmetric arrangement. As a result of a well-organized arrangement, Ogawa et al. (Ogawa and Iwata, 2010) found that the basal spacing got bigger after the sodium exchange in Na-tectosilicate with alkyl-quaternary ammonium in water. This can be simplified as the ODA-soluble solvent (e.g., ethanol) is responsible for the disordered, asymmetric, and unstable conditions of intercalant. In this work, the mixed solvent (Aq/Et 50%) has increased basal spacing due to the abnormal reactivity of the ODA-head tail and the hydroxide functional group of the alumina-silica structure (see Fig. 1b) (Iwasaki, 2020).

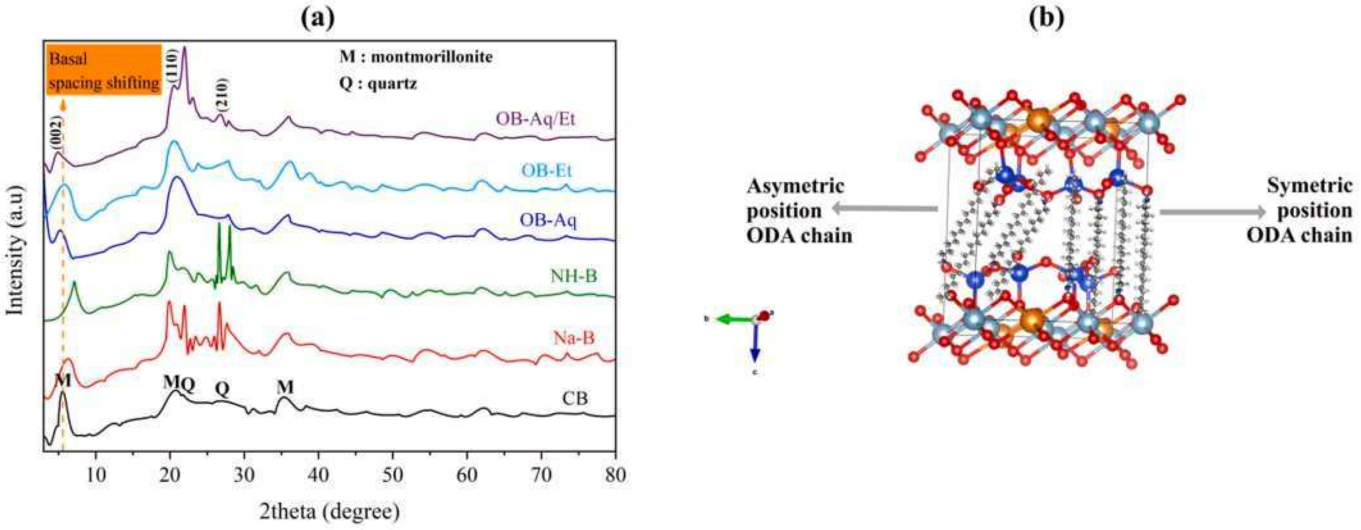

Fig. 1. X-Ray diffraction (XRD) patterns (a) and expected structure arrangement of intercalated ODA (b).

Fourier transform infrared (FTIR) is used for functional group analysis and energy bond detection. For composite materials, FTIR is generally used to confirm the bonding in a plotted graph (Rytwo et al., 2015). In OB, unique adsorption spectra appear at 1404 cm^{-1} and 1465 cm^{-1} as amino group vibrations to the hydroxyl group in the silicate structure (Hakim et al., 2023c). The HT/ST intercalation positively proved that this process is not affected by alumina-silica structure transformation but only by inorganic ion exchange. Additionally, the adsorption peaks at 2846 cm^{-1} and 2916 cm^{-1} indicate the asymmetric and symmetric order for ODA-chain intercalant, respectively (see Fig. 2) (Pedrosa et al., 2020).

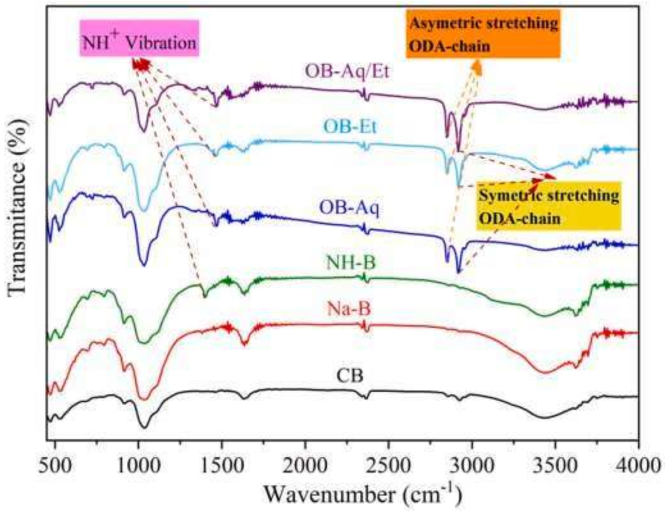

Fig. 2. Fourier transform infrared (FTIR) spectra for fabricated bentonite.

Scanning electron microscopy (SEM) analysis is used to show the morphological structure and other physical properties. The HT/ST intercalation of this OB resulted in expanded and peeled layer phenomena because of the homogenized spread of the intercalant (Ren et al., 2012). Fig. 3 depicts the size of the particle, which is more than 1µm and has an irregular peeled layer structure. Additionally, the use of a polarization solvent helped to modify the roughness of the particles. Thermogravimetry differential thermal analysis (TG-DTA) has a role in thermal stability assessment as a function of structural decomposition (Kok, 2002). Noticeable alterations were detected in the breakdown of the organic phase, which transition to elevated temperatures over 300 °C in OB, referred to as the hydroxylation phase (see Fig. 4). HT/ST intercalation results in a beneficial stability impact for both the individual bentonite components and ODA structures (Kataoka et al., 2019). Furthermore, it was noted that the process of dehydration took place at a temperature of 80 °C.

The regeneration process in DY adsorption also verifies the structural stability when the adsorbent is directly applied. Regeneration refers to the process of reusing an adsorbent after it has undergone an adsorption-desorption cycle. It is a crucial factor in determining the suitability of an adsorbent for practical applications. From an economic standpoint, regeneration greatly decreases the expenses associated with waste treatment, and has the potential to be used in numerous cycles (Liu et al., 2021). The regeneration percentage (%) is referred to in this equation:

$$R\,(\%) = \frac{C0 - C_t}{C_0}\ x\ 100$$

Where, C0 and Ct are initial and specific t-time concentrations in DY adsorption.

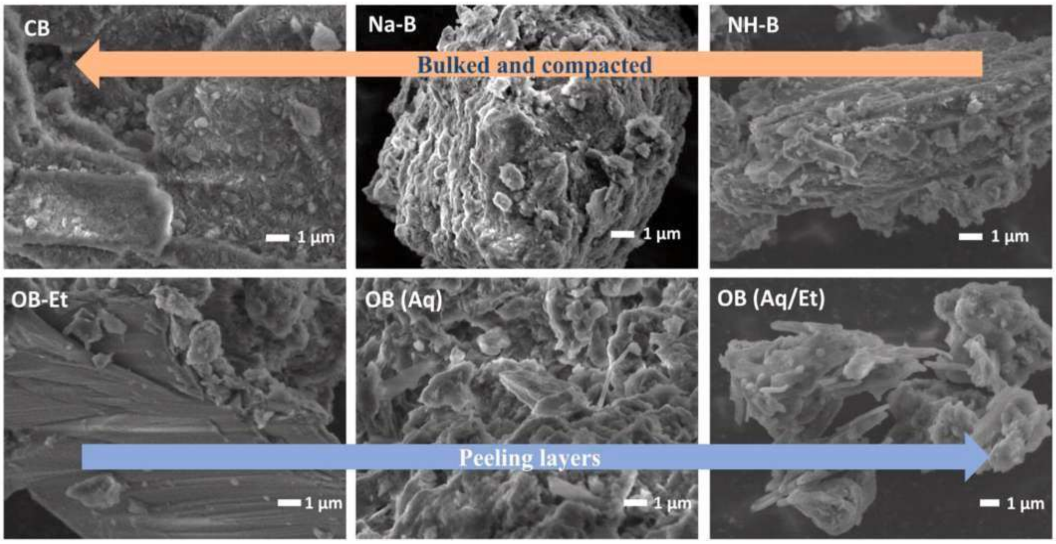

Fig. 3. Morphological photograph of organobentonite.

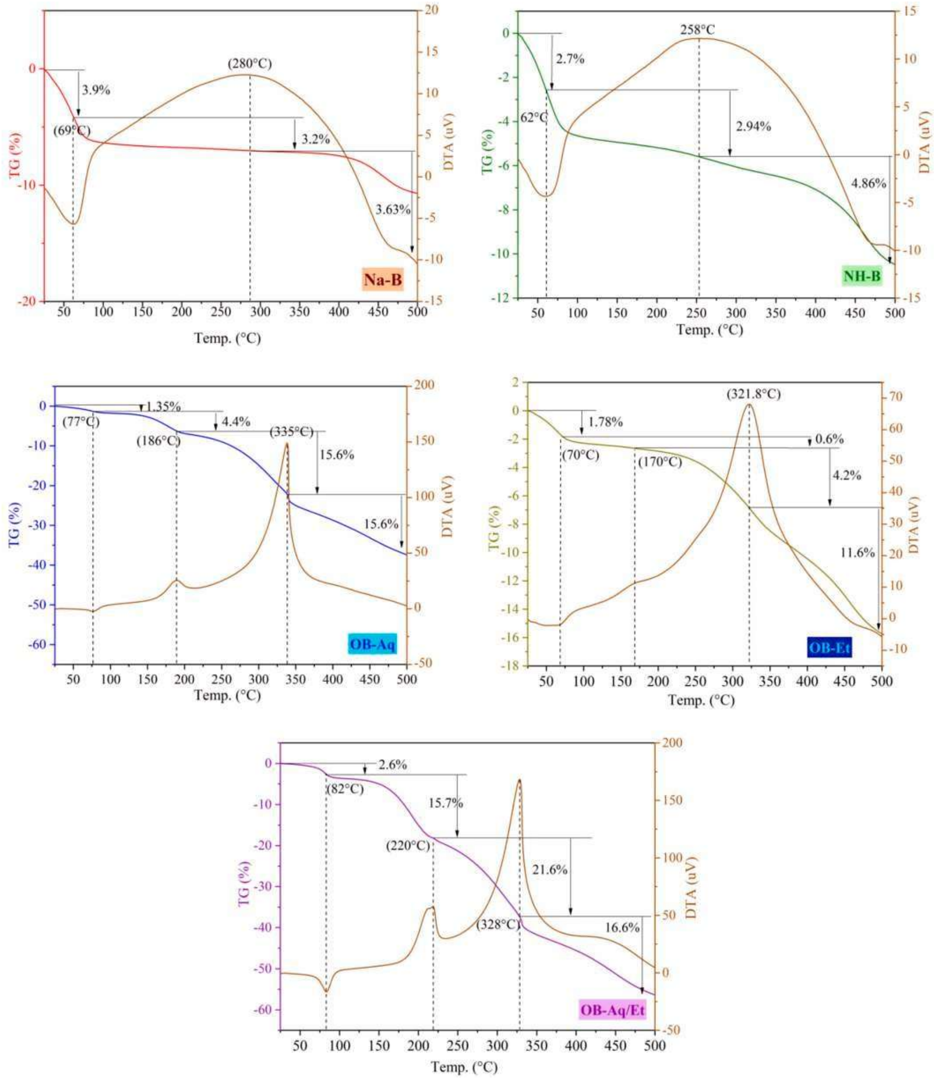

Fig. 4. Thermogravimetry differential thermal analysis (TG-DTA) graph for fabricated organobentonite.

The investigations of the regeneration of the fabricated OB has demonstrated its structural stability, as it exhibited a regeneration per- centage of over 40% after three usage cycles. The regeneration method revealed that the intercalant arrangement structure in OB-Aq/Et is in superior condition. Nevertheless, its efficacy decreased from 93.87% to 71.12% following three rounds of regeneration (see Fig. 5). The stability of the ODA-based OB is attributed to the proportionate connection be- tween the ODA structure within the bentonite layer. This interaction acts as a growth matrix for intercalation. The HT/ST intercalation pathway also induces a strength-anchored effect in ODA intercalation (Yang et al., 2015).

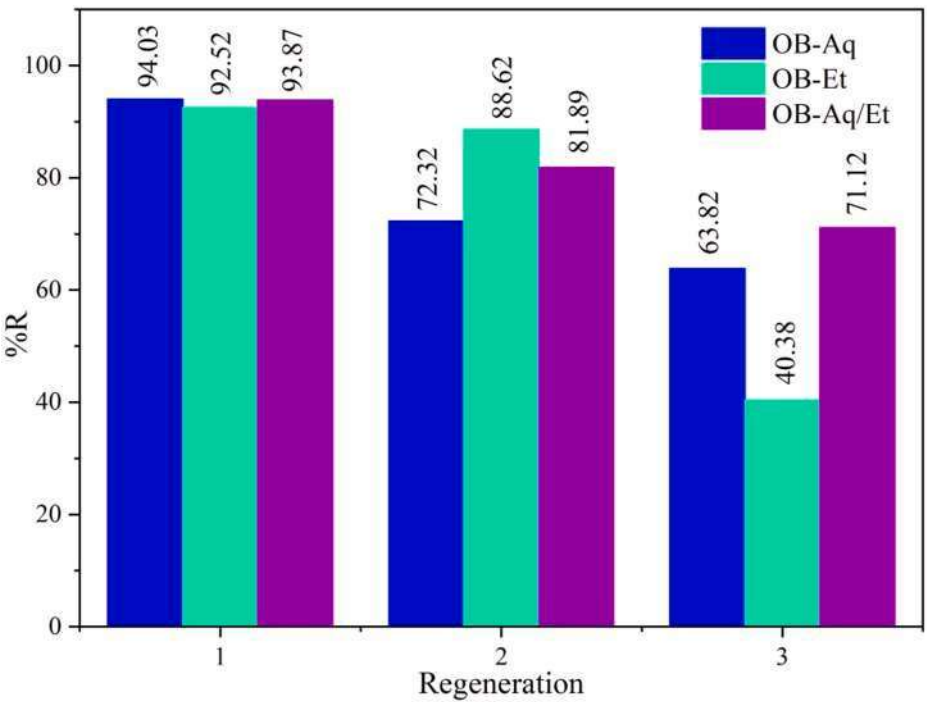

Fig. 5. Regeneration ability of fabricated organobentonite.

Fig. 6 illustrates the adsorption-desorption isotherm of N2 on ODA- based OB. According to the gas adsorption isotherm categorization by IUPAC, the results of this study are categorized as type IV of adsorption isotherm, indicating the presence of mesoporous structures (Brunauer et al., 1940). This is consistent with the findings shown in Table 1, which displays a distinct mesoporous pore diameter ranging from 2 to 50 nm. Nevertheless, OB-Aq and OB-Aq/Et demonstrate a reduction in pore volume and surface area, accompanied by an increase in pore width caused by the occurrence of peeled layers. This observation is supported by the SEM image shown in Fig. 3. The hysteresis loops obtained from type H3 also yield insights into the distribution of pores under non-uniform conditions caused by the composition of granular materials (as confirmed by the SEM photograph) (Yang et al., 2018).

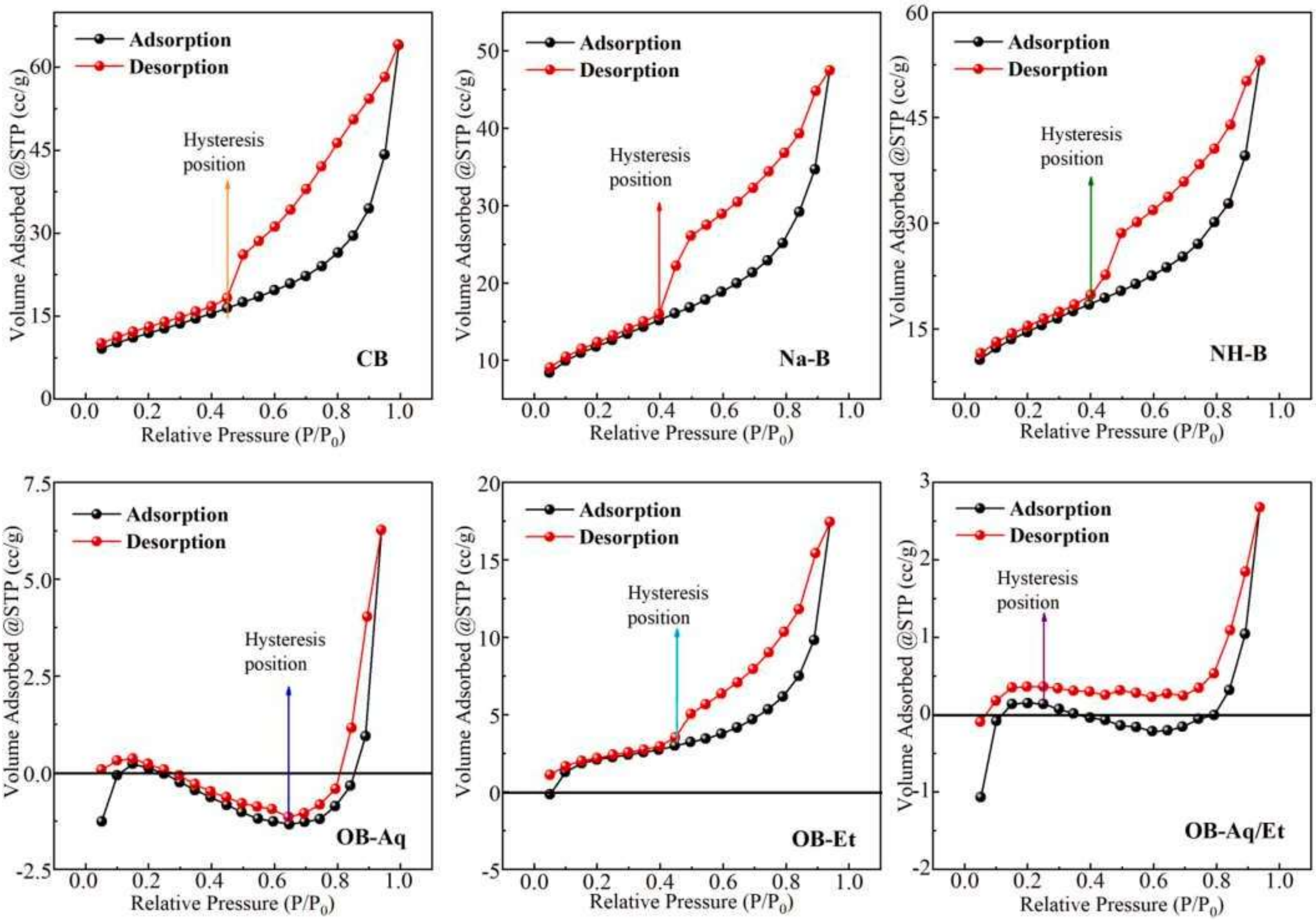

Fig. 6. Adsorption-desorption of N_2 (BET method).

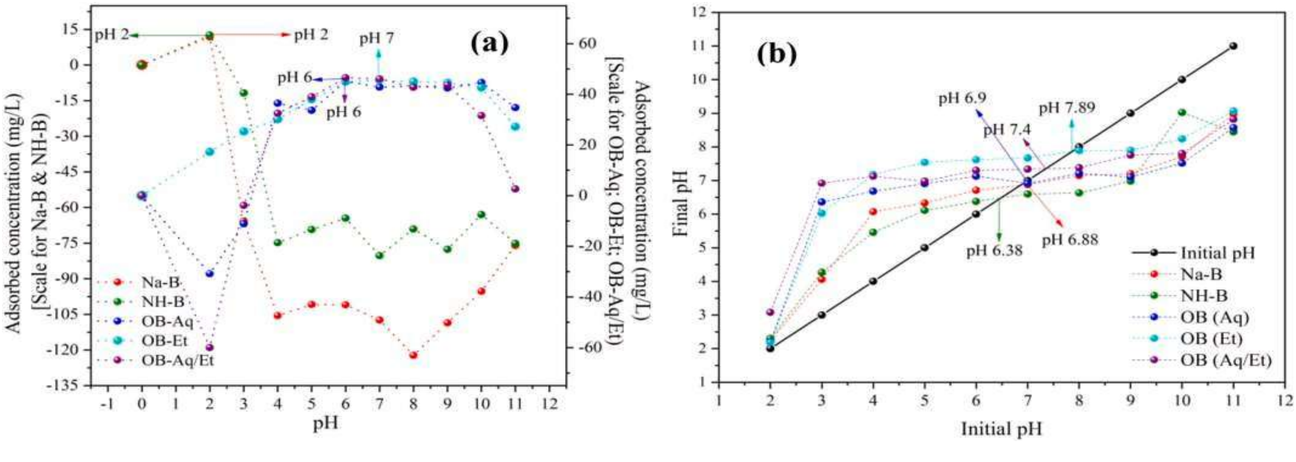

Fig. 7. (A) pH optimum plot and (b) pH_{pzc} analysis.

3.2. *Effect of pH*

The pH level plays a significant role in the adsorption process as it greatly influences the surface charge, the degradation of the adsorbate, and the ionization level of the dye (Hakim et al., 2023b). According to Fig. 7b, pH_{pzc} in OB-Aq, OB-Et, and OB-Aq/Et were 7, 7.8, and 7.25, respectively. The pH values at which the highest adsorption of DY occurred on the adsorbents were 6, 7, and 6, respectively (see Fig. 7a). The optimal pH for adsorbing anionic dyes of DY was suitable for the pH at the point of zero charge (pH_{pzc}), and adjusting the pH eliminated any interference from ions in aqueous solutions. This reasoning adheres to the stipulation that a surface charge will be positive and change direc- tion if the pH optimum is lower than the pH_{pzc} (Priatna et al., 2023), (Nasiruddin Khan et al., 2007). Fig. 8 illustrates the expectation response mechanism, which is associated with the correlation between pH optimal and pH_{pzc} (Kosmulski, 2021).

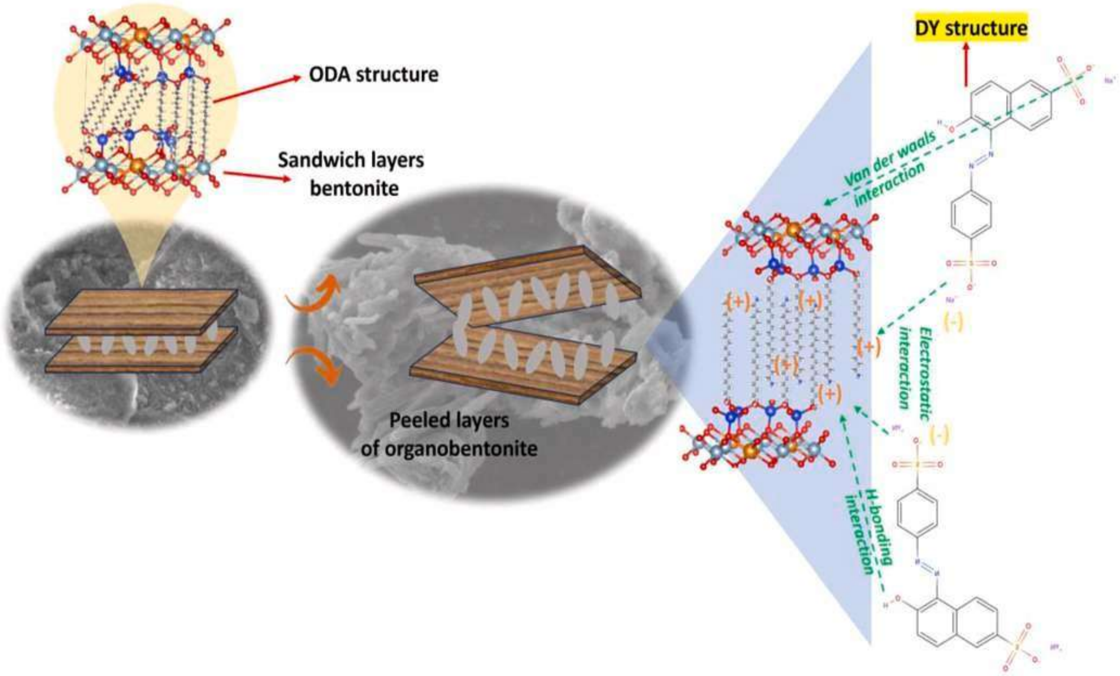

Fig. 8. Reaction mechanism for the direct yellow adsorption. (For interpretation of the references to colour in this figure legend, the reader is referred to the Web version of this article.)

3.3. *Kinetics analysis*

Kinetic analysis has been conducted based on time-variation adsorption. In order for an adsorbent to be suitable, it must have a high adsorption capacity and be able to achieve this in a short amount of time. Therefore, the kinetic parameters are evaluated using several models such as the pseudo-first-order (PFO), pseudo-second-order (PSO), intraparticle diffusion, and Elovich models (Hakim et al., 2023b), (Dada et al., 2021). The PFO kinetic model is used to analyze the OB-Aq, OB-Et, and OB-Aq/Et. This model explains the adsorption pro- cess by considering the proportional composition between the number of active sites on the adsorbent and the demand rate of the removal site (see Fig. 9 and Table 2) (Hakim et al., 2023a). However, when the quantity of active site adsorbents surpasses the quantity of molecules in the adsorbate, PSO models will be created according to the chemisorp- tion scheme (Lalji et al., 2022). The PFO models elucidate that adsorp- tion takes place uniformly over the surfaces of the adsorbent under a constant temperature condition. This explanation aligns with the SEM photograph of porous structure materials, which serves as the sites for the reaction.

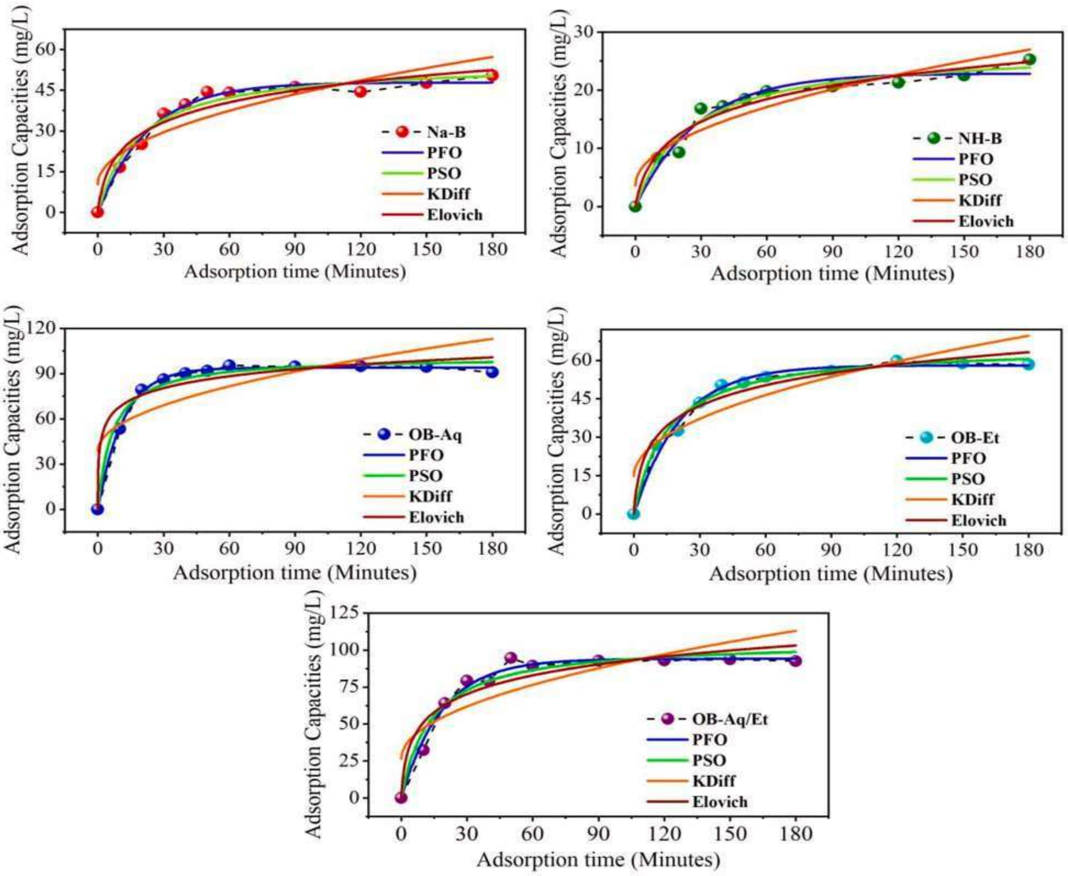

Fig. 9. Plot for kinetic parameters of direct yellow adsorption. (For interpretation of the references to colour in this figure legend, the reader is referred to the Web version of this article.

3.4. *Isotherm and thermodynamics analyses*

The Langmuir, Freundlich, Temkin, and Dubinin-Raduskevich isotherm models determine the expected mechanism and intensity of the interaction between the adsorbate and adsorbent by utilizing isotherm parameters (Wang and Guo, 2020). Table 3 presents the comparative outcomes for the adsorption of DY in several isotherm models. Additionally, OB adsorbents of OB-Aq, OB-Et, and OB-Aq/Et were fitted to the Langmuir model based on the consistency of the R^2 value. This model explains the adsorption process, which takes place in a monolayer area (identical and equivalent number of adsorbate molecules to the definite localized sites of the adsorbent) or chemisorption (Langmuir, 1918), (Langmuir, 1916). Temperature has a crucial role in determining the adsorption capabilities by influencing molecular interactions (Hakim et al., 2023a). The maximum capacities (Q_{max}) of Na–B, NH–B, OB-Aq, OB-Et, and OB-Aq/Et were 625 mg/g, 158.73 mg/g, 270.27 mg/g, 108.696 mg/g, and 2000 mg/g, respectively. Table 4 presents a comparison of the efficacy of this study's elimination of DY for OB in relation to prior findings. These lists are created based on several adsorbent uses, using a representative pollutant (DY), in order to compare the efficiency of the adsorption process. The study clearly demonstrates that OB products exhibit superior removal of DY dyes as a result of a higher Q_{max}.

Thermodynamic parameters are utilized to determine the sponta- neity and thermodynamic impacts of heat change. Enthalpy (ΔH) and entropy (ΔS) were both utilized as crucial variables in the calculation of
the Gibbs free energy (ΔG). The adsorption process generally follows endothermic conditions according to the positive value of ΔH (see Table 5) (Hakim et al., 2023a). The positive value of ΔS indicates an increase in unpredictability resulting from the affinity between the adsorbate and adsorbent at higher temperatures (Al-Ghouti and Da'ana, 2020). Furthermore, the variations in ΔG for Na–B, NH–B, OB-Aq, and OB-Aq/Et are negative, indicating spontaneous adsorption reactions.

Consequently, these conditions greatly enhance the ability of the adsorbent to attract and hold molecules by increasing the temperature and reducing repulsive forces on its surface.

4. Conclusion

This work proposed the organobentonite (OB) fabrication assisted by intercalation of surfactant octadecylamine under hydrothermal/sol- vothermal conditions (solvents: distilled water (OB-Aq), ethanol (OB–Et), and 50% mix:ethanol (OB-Aq/Et)). Hydrothermal/sol- vothermal intercalation caused an increase in the distance between the layers of bentonite, resulting in the separation of these layers and the formation of mesopores, which facilitated the adsorption of direct yel- low. The structural stability of the material was verified using thermal treatment, which demonstrated resistance at temperatures over 300 °C. Additionally, the material's ability to be regenerated was assessed and shown to be efficient for up to three cycles. The chemisorption mechanism resulted in the maximum adsorption capacity of OB-Aq, OB-Et, and OB-Aq/Et at 270.27 mg/g, 108.696 mg/g, and 2000 mg/g, respectively. This work provides a method for assessing organobentonite adsorbents in wastewater treatment, including optimal removal conditions. The results of this work are also significant for the hydrothermal/sol- vothermal production of high-capacity, environmentally acceptable bentonite-based adsorbents for anionic dyes.

Declaration of competing interest

The authors declare that they have no known competing financial

Acknowledgments

The authors acknowledge the funding support from PMDSU (Pen- didikan Magister menuju Doktor untuk Sarjana Unggul) scholarship's grant No. 0195.02/UN9.3.1/PL/2023 under the Ministry of Education, Culture, Research, and Technology of the Republic of Indonesia. Furthermore, the author appreciates the Research Centre of Inorganic Materials and Complexes Laboratory of Sriwijaya University and the Environmental Inorganic Materials Chemistry Laboratory of the Insti- tute for Multidisciplinary Research for Advanced Materials, Tohoku University, for instrumentation support.

Credit autorship contribution statement

Yusuf Mathiinul Hakim: Data curation, Formal analysis, Investi- gation, Methodology, Resources, Software, Validation, Visualization, Writing – original draft, Writing – review & editing. **Mardiyanto:** Conceptualization, Formal analysis, Supervision, Validation. **Idha Royani:** Formal analysis, Resources, Supervision. **Risfidian Mohadi:** Writing – review & editing, Conceptualization, Formal analysis, Funding acquisition, Project administration, Resources, Supervision.

Acknowledgments

The authors acknowledge the funding support from PMDSU (Pen- didikan Magister menuju Doktor untuk Sarjana Unggul) scholarship's grant No. 0195.02/UN9.3.1/PL/2023 under the Ministry of Education, Culture, Research, and Technology of the Republic of Indonesia. Furthermore, the author appreciates the Research Centre of Inorganic Materials and Complexes Laboratory of Sriwijaya University and the Environmental Inorganic Materials Chemistry Laboratory of the Insti- tute for Multidisciplinary Research for Advanced Materials, Tohoku University, for instrumentation support.

Credit autorship contribution statement

Yusuf Mathiinul Hakim: Data curation, Formal analysis, Investi- gation, Methodology, Resources, Software, Validation, Visualization, Writing – original draft, Writing – review & editing. **Mardiyanto:** Conceptualization, Formal analysis, Supervision, Validation. **Idha Royani:** Formal analysis, Resources, Supervision. **Risfidian Mohadi:** Writing – review & editing, Conceptualization, Formal analysis, Funding acquisition, Project administration, Resources, Supervision.

References

Ahmad, N., Suryani Arsyad, F., Royani, I., Lesbani, A., 2023. Charcoal activated as template Mg/Al layered double hydroxide for selective adsorption of direct yellow Adsorbent Conc.on anionic dyes. Results Chem 5, 100766. https://doi.org/10.1016/j. rechem.2023.100766.

Al-Ghouti, M.A., Da’ana, D.A., 2020. Guidelines for the use and interpretation of adsorption isotherm models: a review. J. Hazard Mater. 393 https://doi.org/ 10.1016/j.jhazmat.2020.122383. Elsevier B.V.

Alabbad, E.A., 2021. Efficacy assessment of natural zeolite containing wastewater on the adsorption behaviour of Direct Yellow 50 from; equilibrium, kinetics and thermodynamic studies. Arab. J. Chem. 14 (4), 103041 https://doi.org/10.1016/j. arabjc.2021.103041.

Alabbad, E.A., 2023. Effect of Direct yellow 50 removal from an aqueous solution using nano bentonite; adsorption isotherm, kinetic analysis and also thermodynamic behavior. Arab. J. Chem. 16 (2), 104517 https://doi.org/10.1016/j. arabjc.2022.104517.

Alzain, H., Kalimugogo, V., Hussein, K., 2023. A review of environmental impact of azo dyes. International Journal of Research and Review 10 (6), 64–689. https://doi.org/ 10.52403/ijrr.20230682.

Ayisha Sidiqua, M., Priya, V.S., 2021. Removal of yellow dye using composite binded adsorbent developed using natural clay and activated carbon from sapindus seed. Biocatal. Agric. Biotechnol. 33, 101965 https://doi.org/10.1016/j. bcab.2021.101965.

Barakan, S., Aghazadeh, V., 2021. The advantages of clay mineral modification methods for enhancing adsorption efficiency in wastewater treatment: a review. Environ. Sci Pollut. Control Ser. 28 (3), 2572–2599. https://doi.org/10.1007/s11356-020-10985-9.

Brunauer, S., Deming, L.S., Deming, W.E., Teller, E., 1940. On a Theory of the van der Waals Adsorption of Gases. J. Am. Chem. Soc. 62 (7), 1723–1732. https://doi.org/ 10.1021/ja01864a025.

Çalıs¸kan Salihi, E., Cantürk Talman, R.Y., Go¨ktürk, S., 2023. Preparation and characterization of surfactant loaded clays as drug adsorbents. J Dispers Sci Technol 44 (1), 165–173. https://doi.org/10.1080/01932691.2021.1931289.

Cuevas, J., et al., 2022. Bentonite Powder XRD Quantitative analysis using Rietveld Refinement: Revisiting and updating bulk semiquantitative mineralogical compositions. Minerals 12 (6), 772. https://doi.org/10.3390/min12060772.

Dada, A.O., Adekola, F.A., Odebunmi, E.O., Ogunlaja, A.S., Bello, O.S., 2021. Two–three parameters isotherm modeling, kinetics with statistical validity, desorption and thermodynamic studies of adsorption of Cu(II) ions onto zerovalent iron nanoparticles. Sci. Rep. 11 (1), 16454 https://doi.org/10.1038/s41598-021-95090-8.

Dadou, S., Berrama, T., Doufene, N., Zekkaoui, C., Beriber, A., 2019. Evaluating untreated clay's adsorptive capacity to remove an anionic dye from aqueous solution. Arab J Sci Eng 44 (12), 9889–9903. https://doi.org/10.1007/s13369-019-04100-5.

de Morais Pinos, J.Y., de Melo, L.B., de Souza, S.D., Marçal, L., de Faria, E.H., 2022. Bentonite functionalized with amine groups by the sol-gel route as efficient adsorbent of rhodamine-B and nickel (II). Appl. Clay Sci. 223, 106494 https://doi.org/10.1016/j.clay.2022.106494.

Feng, S.-H., Li, G.-H., 2017. Hydrothermal and solvothermal syntheses. In: Modern Inorganic Synthetic Chemistry. Elsevier, pp. 73–104. https://doi.org/10.1016/B978- 0-444-63591-4.00004-5.

Garg, A., Chopra, L., 2022. Dye Waste: a significant environmental hazard. Mater Today Proc 48, 1310–1315. https://doi.org/10.1016/j.matpr.2021.09.003.

Hajati, S., Ghaedi, M., Karimi, F., Barazesh, B., Sahraei, R., Daneshfar, A., 2014.

Competitive adsorption of Direct Yellow 12 and Reactive Orange 12 on ZnS:Mn nanoparticles loaded on activated carbon as novel adsorbent. J. Ind. Eng. Chem. 20 (2), 564–571. https://doi.org/10.1016/j.jiec.2013.05.015.

Hakim, Y.M., Royani, I., Mardiyanto, M., Mohadi, R., 2023a. Bentonite impregnation
ammonium-assisted as eco-friendly dye adsorbent: analyses of kinetics and thermodynamics in cationic dye adsorption. Key Eng. Mater. 963, 85–102. https://doi.org/10.4028/p-0UEtzJ.

Hakim, Y., Mohadi, R., Mardiyanto, M., Royani, I., 2023b. Ammonium-assisted intercalation of java bentonite as effective of cationic dye removal. Journal of Ecological Engineering 24 (2), 184–195. https://doi.org/10.12911/22998993/156665.

Hakim, Y.M., Khakim, M.Y.N., Hanifah, A., Mohadi, R., 2023c. Optimization of sumatera bentonite by ammonium-impregnated as a coagulant for cassava wastewater treatment. Science and Technology Indonesia 8 (3), 443–450. https://doi.org/10.26554/sti.2023.8.3.443-450.

Hemashenpagam, N., Selvajeyanthi, S., 2023. Textile Dyes and Their Effect on Human Beings, pp. 41–60. https://doi.org/10.1007/978-981-99-3901-5_3.

Iwasaki, T., 2020. Effect of solvents on the direct intercalation of decylamine into H-octosilicate. Appl. Clay Sci. 199, 105882 https://doi.org/10.1016/j. clay.2020.105882.

Kataoka, T., Shiba, K., Nagata, S., Yamada, I., Tagaya, M., 2019. Effects of surfactant removal processes from titania/octadecylamine hybrid particles on their nanostructures and dispersibility in phosphate buffered saline. Results Phys. 13, 102215 https://doi.org/10.1016/j.rinp.2019.102215.

Khezrianjoo, S., 2019. Photodestruction of Direct Yellow 11 in aqueous TiO2 suspension: effect of operational parameters on detoxification, Langmuir–Hinshelwood kinetic expression and biodegradability. Desalination Water Treat. 153, 264–278. https://doi.org/10.5004/dwt.2019.23766.

Kok, M.V., 2002. Thermogravimetry of selected bentonites. Energy Sources 24 (10), 907–914. https://doi.org/10.1080/00908310290086833.

Kosmulski, M., 2021. The pH dependent surface charging and points of zero charge. IX. Update. Adv. Colloid Interface Sci. 296, 102519 https://doi.org/10.1016/j.

cis.2021.102519.

Laipan, M., et al., 2020. Layered intercalation compounds: mechanisms, new methodologies, and advanced applications. Prog. Mater. Sci. 109, 100631 https://doi.org/10.1016/j.pmatsci.2019.100631.

Lalji, S.M., Ali, S.I., Ahmed, R., Hashmi, S., Awan, Z.U.H., 2022. Comparative performance analysis of different swelling kinetic models for the evaluation of shale swelling. J. Pet. Explor. Prod. Technol. 12 (5), 1237–1249. https://doi.org/10.1007/s13202-021-01387-9.

Langmuir, I., 1916. The constitution and fundamental properties of solids and liquids. Part I. Solids. J. Am. Chem. Soc. 38 (11), 2221–2295. https://doi.org/10.1021/ja02268a002.

Langmuir, I., 1918. The adsorption of gases on plane surfaces of glass, mica and platinum. J. Am. Chem. Soc. 40 (9), 1361–1403. https://doi.org/10.1021/ ja02242a004.

Liu, X., et al., 2021. Modification of sugar-based carbon using lanthanum and cobalt bimetal species for effective adsorption of methyl orange. Environ. Technol. Innov. 23, 101769 https://doi.org/10.1016/j.eti.2021.101769.

Mahmood, S., Mahmood, S., Mahmood, S., 2014. Adsorption/desorption of Direct Yellow 28 on apatitic phosphate: mechanism, kinetic and thermodynamic studies. Journal of the Association of Arab Universities for Basic and Applied Sciences 16 (1), 64–73.https://doi.org/10.1016/j.jaubas.2013.09.001.

Mir, A.A.-, Amooey, A.A., Ghasemi, S., 2018. Adsorption of direct yellow 12 from aqueous solutions by an iron oxide-gelatin nanoadsorbent; kinetic, isotherm and mechanism analysis. J. Clean. Prod. 170, 570–580. https://doi.org/10.1016/j.jclepro.2017.09.101.

Nasiruddin Khan, M., Sarwar, A., Research Centre, F., Karachi, P., 2007. Determination of points of zero charge of natural and treated adsorbents [Online]. Available: www. worldscientific.com.

Ogawa, M., Iwata, D., 2010. Arrangements of interlayer quaternary ammonium ions in a layered silicate, octosilicate. Cryst. Growth Des. 10 (5), 2068–2072. https://doi.org/ 10.1021/cg900922v.

Pedrosa, M.C.G., Dutra Filho, J.C., de Menezes, L.R., da Silva, E.O., 2020. Chemical surface modification and characterization of carbon nanostructures without shape damage. Mater. Res. 23 (2) https://doi.org/10.1590/1980-5373-mr-2019-0493.

Priatna, S.J., Hakim, Y.M., Alfarizi, M.A., Sailah, S., Mohadi, R., 2023. Palm oil mill effluent (POME) precipitation using ammonium-intercalated clay coagulant. Communications in Science and Technology 8 (1), 10–15. https://doi.org/ 10.21924/cst.8.1.2023.1034.

Qi, J., Yu, J., Shah, K.J., Shah, D.D., You, Z., 2023. Applicability of clay/organic clay to environmental pollutants: green way—an overview. Appl. Sci. 13 (16), 9395. https://doi.org/10.3390/app13169395.

Rashid, R., Shafiq, I., Akhter, P., Iqbal, M.J., Hussain, M., 2021. A state-of-the-art review on wastewater treatment techniques: the effectiveness of adsorption method. Environ. Sci. Pollut. Control Ser. 28 (8), 9050–9066. https://doi.org/10.1007/ s11356-021-12395-x.

Ren, L., et al., 2012. Large-scale production of ultrathin topological insulator bismuth telluride nanosheets by a hydrothermal intercalation and exfoliation route. J. Mater. Chem. 22 (11), 4921. https://doi.org/10.1039/c2jm15973b.

Rytwo, G., Zakai, R., Wicklein, B., 2015. The use of ATR-FTIR spectroscopy for quantification of adsorbed compounds. Journal of Spectroscopy 2015, 1–8. https:// doi.org/10.1155/2015/727595.

Scheufele, F.B., et al., 2016. Monolayer–multilayer adsorption phenomenological model: kinetics, equilibrium and thermodynamics. Chem. Eng. J. 284, 1328–1341. https://doi.org/10.1016/j.cej.2015.09.085.

Segad, M., Jo¨nsson, B., Åkesson, T., Cabane, B., 2010. Ca/Na montmorillonite: structure, forces and swelling properties. Langmuir 26 (8), 5782–5790. https://doi.org/ 10.1021/la9036293.

Taibi, Z., et al., 2023. Adsorption of orange G dye on hydrophobic activated bentonite from aqueous solution. Crystals 13 (2), 211. https://doi.org/10.3390/ cryst13020211.

Tozer, L., 2023. Water pollution 'timebomb' threatens global health. Nature. https://doi.org/10.1038/d41586-023-02337-7.

UNESCO World Water Assessment Programme, Koncagul, E., Connor, R., 2023. The united nations world water development report 2023: partnerships and cooperation for water; facts, figures and action examples [Online]. Available. https://unesdoc.unesco.org/ark:/48223/pf0000384659. (Accessed 15 March 2024).

Vats, S., et al., 2022. Advances in dye contamination. In: Biological Approaches to Controlling Pollutants. Elsevier, pp. 139–162. https://doi.org/10.1016/B978-0-12- 824316-9.00020-3.

Wang, J., Guo, X., 2020. Adsorption isotherm models: classification, physical meaning, application and solving method. Chemosphere 258, 127279. https://doi.org/ 10.1016/j.chemosphere.2020.127279.

Yang, C., Zhu, Y., Wang, J., Li, Z., Su, X., Niu, C., 2015. Hydrothermal synthesis of TiO2–WO3–bentonite composites: conventional versus ultrasonic pretreatments and their adsorption of methylene blue. Appl. Clay Sci. 105–106, 243–251. https://doi. org/10.1016/j.clay.2015.01.002.

Yang, S., et al., 2018. Evolution of nanopore structure in lacustrine organic-rich shales during thermal maturation from hydrous pyrolysis, Minhe Basin, Northwest China. Energy Explor. Exploit. 36 (2), 265–281. https://doi.org/10.1177/0144598717723647.

Yaqoub, E., 2023. Water Resources management crisis in Palestine. In: The Handbook of Environmental Chemistry, pp. 1–13. https://doi.org/10.1007/698_2023_975.

Zhong, H., et al., 2022. Hydrothermal synthesis of bentonite carbon composites for ultra- high temperature filtration control in water-based drilling fluid. Appl. Clay Sci. 230, 106699 https://doi.org/10.1016/j.clay.2022.106699.

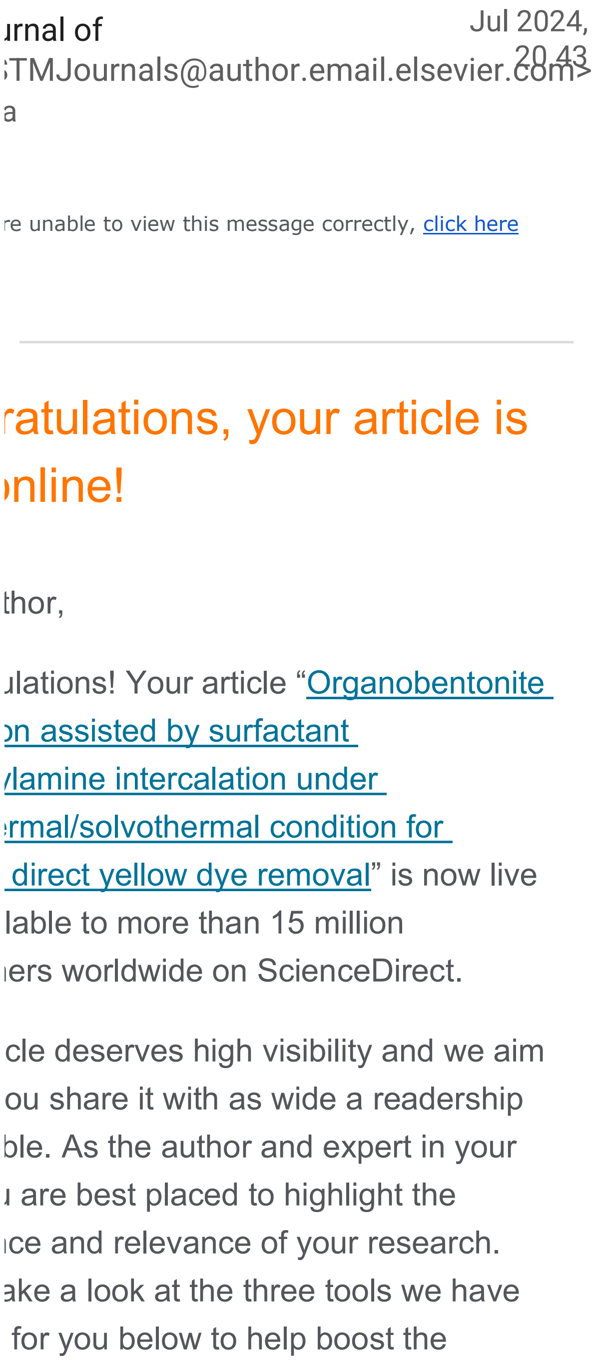

ırnal of
ΐTMJournals@author.email.elsevier.com>
a

Jul 2024,
20 43

re unable to view this message correctly, click here

ratulations, your article is
online!

thor,

ılations! Your article “Organobentonite
on assisted by surfactant
ylamine intercalation under
ermal/solvothermal condition for
direct yellow dye removal” is now live
lable to more than 15 million
ıers worldwide on ScienceDirect.

cle deserves high visibility and we aim
ou share it with as wide a readership
ble. As the author and expert in your
ı are best placed to highlight the
ıce and relevance of your research.
ake a look at the three tools we have
for you below to help boost the

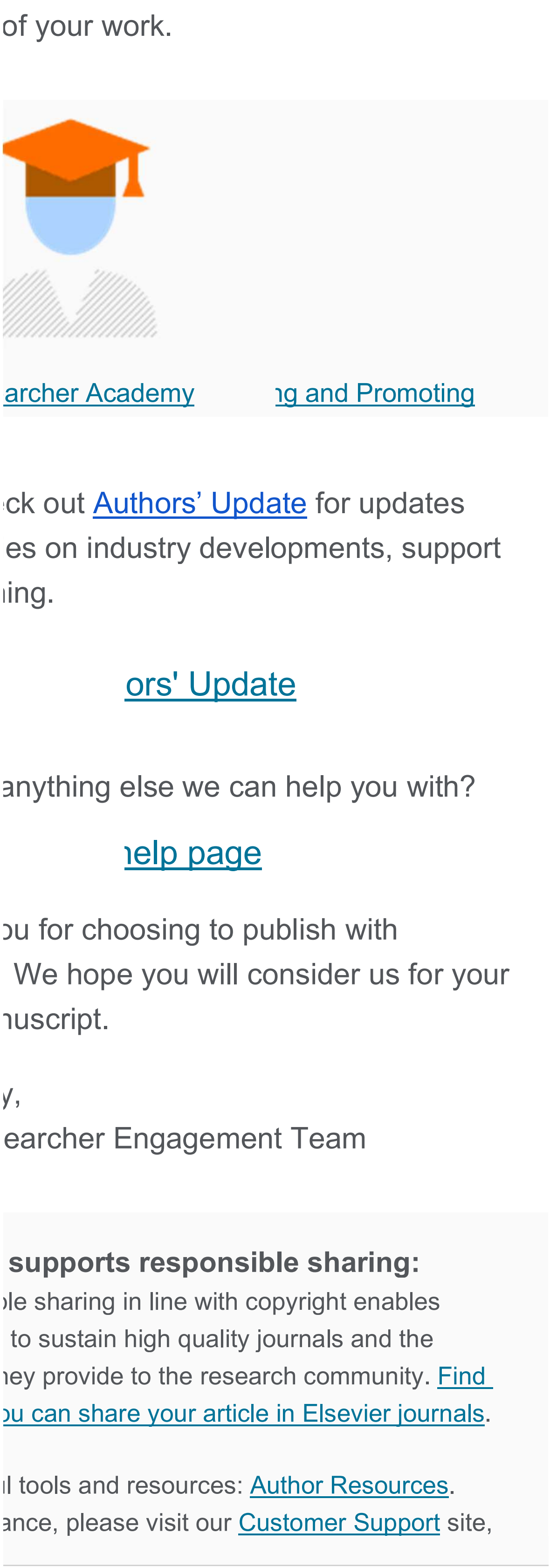

of your work.

archer Academy ıg and Promoting

ːck out Authors’ Update for updates
es on industry developments, support
ıing.

ors' Update

anything else we can help you with?

ıelp page

ɔu for choosing to publish with
We hope you will consider us for your
ıuscript.

y,
earcher Engagement Team

supports responsible sharing:
ɔle sharing in line with copyright enables
to sustain high quality journals and the
ıey provide to the research community. Find
ɔu can share your article in Elsevier journals.

ıl tools and resources: Author Resources.
ance, please visit our Customer Support site,

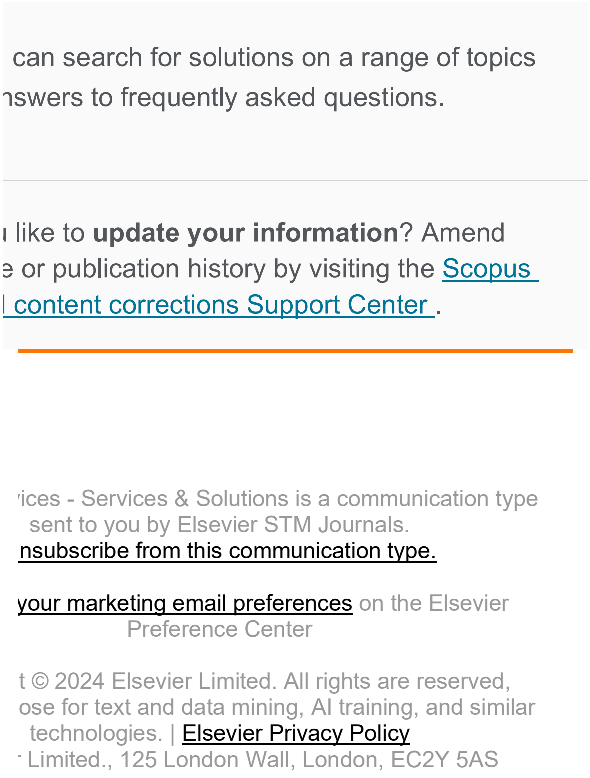

can search for solutions on a range of topics
ıswers to frequently asked questions.

ı like to **update your information**? Amend
e or publication history by visiting the Scopus
l content corrections Support Center .

ices - Services & Solutions is a communication type
sent to you by Elsevier STM Journals.
nsubscribe from this communication type.

your marketing email preferences on the Elsevier
Preference Center

t © 2024 Elsevier Limited. All rights are reserved,
ose for text and data mining, AI training, and similar
technologies. | Elsevier Privacy Policy
Limited., 125 London Wall, London, EC2Y 5AS